Prediction of absolute crystal-nucleation rate in hard-sphere colloids

Stefan Auer & Daan Frenkel

FOM Institute for Atomic and Molecular Physics, Kruislaan 407, 1098 SJ Amsterdam, The Netherlands

Crystal nucleation is a much-studied phenomenon, yet the rate at which it occurs remains difficult to predict. Small crystal nuclei form spontaneously in supersaturated solutions, but unless their size exceeds a critical value—the so-called critical nucleus—they will re-dissolve rather than grow. It is this rate-limiting step that has proved difficult to probe experimentally. The crystal nucleation rate depends on P_{crit}, the (very small) probability that a critical nucleus forms spontaneously, and on a kinetic factor (κ) that measures the rate at which critical nuclei subsequently grow. Given the absence of *a priori* knowledge of either quantity, classical nucleation theory[1] is commonly used to analyse crystal nucleation experiments, with the unconstrained parameters adjusted to fit the observations. This approach yields no 'first principles' prediction of absolute nucleation rates. Here we approach the problem from a different angle, simulating the nucleation process in a suspension of hard colloidal spheres, to obtain quantitative numerical predictions of the crystal nucleation rate. We find large discrepancies between the computed nucleation rates and those deduced from experiments[2–4]: the best experimental estimates of P_{crit} seem to be too large by several orders of magnitude.

The probability (per particle) that a spontaneous fluctuation will result in the formation of a critical nucleus depends exponentially on the free energy ΔG_{crit} that is required to form such a nucleus:

$$P_{crit} = \exp(-\Delta G_{crit}/k_B T) \quad (1)$$

where T is the absolute temperature and k_B is Boltzmann's constant. According to classical nucleation theory (CNT), the total free energy of a crystallite that forms in a supersaturated solution contains two terms: the first is a 'bulk' term that expresses the fact that the solid is more stable than the supersaturated fluid—this term is negative and proportional to the volume of the crystallite. The second is a 'surface' term that takes into account the free-energy cost of creating a solid–liquid interface. This term is positive and proportional to the surface area of the crystallite. According to CNT, the total (Gibbs) free-energy cost to form a spherical crystallite with radius R is

$$\Delta G = \frac{4}{3}\pi R^3 \rho_S \Delta\mu + 4\pi R^2 \gamma \quad (2)$$

where ρ_S is the number-density of the solid, $\Delta\mu$ (<0) is the difference in chemical potential of the solid and the liquid, and γ is the solid–liquid interfacial free energy density. The function ΔG goes through a maximum at $R = 2\gamma/(\rho_S|\Delta\mu|)$ and the height of the nucleation barrier is:

$$\Delta G_{crit} = \frac{16\pi}{3}\gamma^3/(\rho_S|\Delta\mu|)^2 \quad (3)$$

The crystal-nucleation rate per unit volume, I, is the product of P_{crit} and the kinetic prefactor κ:

$$I = \kappa \exp(-\Delta G_{crit}/k_B T) \quad (4)$$

The CNT expression for the nucleation rate then becomes:

$$I = \kappa \exp\left[-\frac{16\pi}{3}\gamma^3/(\rho_S|\Delta\mu|)^2\right] \quad (5)$$

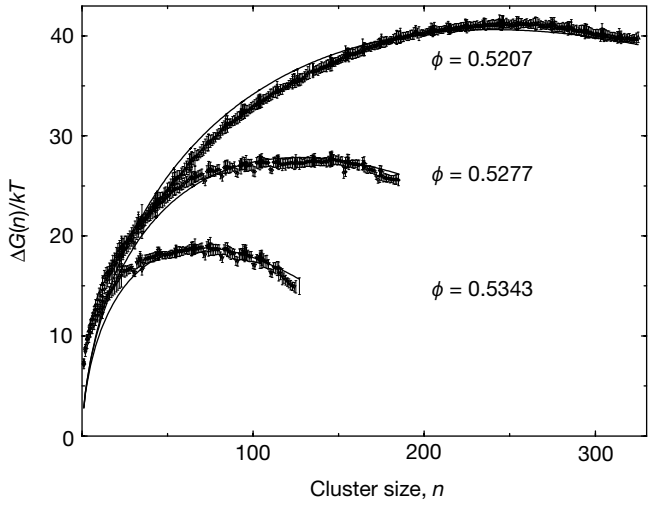

Figure 1 The calculated free-energy barrier for homogeneous crystal nucleation of hard-sphere colloids. Results are shown for three values of the volume fraction of the colloids in the liquid phase. $\phi_{liq} = 0.5207$, 0.5277 and 0.5343. The barrier was computed using equation (6). A prerequisite for the calculation of the nucleation barrier is the choice of a 'reaction coordinate' that measures the progress from liquid to solid. As our reaction coordinate we use n, the number of particles that constitute the largest solid-like cluster in the system. A criterion based on that in ref. 8 was used to identify which particles are solid-like. If two solid-like particles are less than 2σ apart, where σ is the diameter of a particle, then they are counted as belonging to the same cluster. Using this technique we are able to distinguish between particles in a liquid-like environment and particles that belong to crystalline nuclei. For all but the smallest clusters, $P(n) \ll 1$. We used 'umbrella sampling'[22] to determine $P(n)$ in the range where it is very small. The total simulation was split up into a number of smaller simulations that were restricted to a sequence of narrow, but overlapping 'windows' of n values. Stacking rearrangements in the crystalline nuclei were found to be slow. To alleviate this problem, we applied the parallel tempering scheme of Geyer and Thompson[23] to exchange clusters between adjacent windows. All simulations were performed at constant pressure and with the total number of particles (solid plus liquid) fixed. For every window, the simulations took at least 8×10^5 Monte Carlo moves per particle, excluding equilibration. The results of all simulations are presented in reduced units. In all cases, periodic boundary conditions were imposed. To eliminate noticeable finite-size effects, we simulated systems containing 3,375 hard spheres. The drawn curves are fits to the CNT expression (equation (2)). The fits yield the following values: $\gamma_{eff}(P = 15) = 0.699$, $\gamma_{eff}(P = 16) = 0.738$ and $\gamma_{eff}(P = 17) = 0.748$.

This expression has been used extensively to analyse crystal-nucleation experiments. However, as a rigorous theory for the kinetic prefactor is lacking, CNT has not been very successful in predicting absolute nucleation rates. Rather, the kinetic prefactor κ and, more often than not, the effective interfacial free energy γ are fitted to match the experimental nucleation rates[1]. This situation is now changing. The computer simulations that we report here allow us to predict absolute crystal nucleation rates without making use of any adjustable fit parameters or, for that matter, of the assumptions underlying CNT. It is obviously important to compare the simulation results with crystal-nucleation experiments on a system that is very well characterized. For this reason, we chose to simulate crystal nucleation in suspensions of hard-sphere colloids. The hard-sphere freezing transition is probably better characterized than any other. Moreover, several groups have performed experimental studies of crystal nucleation in suspensions of hard-sphere colloids[2–5].

Experimental nucleation rate densities are usually expressed in dimensionless form: $I^\star \equiv I\sigma^5/D_0$. Here σ is the hard-core diameter of the colloidal particles and D_0 is their self-diffusion coefficient at infinite dilution. In what follows, we always use reduced quantities and hence we will omit the asterisk. We use σ as our unit of length, k_BT as our unit of energy and σ^2/D_0 as our unit of time. In the analysis of experiments on hard-core colloids, the kinetic prefactor κ is usually written as $A\phi_{liq}^{5/3}D(\phi_{liq})$, where ϕ_{liq} is the volume fraction of the colloids in the liquid phase, $D(\phi)$ is the (known) reduced diffusivity at volume fraction ϕ, while A and γ are treated as adjustable parameters[3,4,6]. We note that, even apart from the use of adjustable parameters to fit the data, the experimental tests of CNT for hard-sphere freezing are, at present, rather indirect as experiments do not probe the shape of the nucleation barrier directly. Nor do they provide information about the structure of the critical nucleus.

We have performed numerical simulations of hard-sphere colloids that allow us to compute the shape and height of the nucleation barrier and the structure of the critical nucleus. In addition, we have performed kinetic Monte Carlo simulations to compute the kinetic prefactor κ. These allow us to compare our simulation results for the reduced nucleation rate (without adjustable parameters) with the values of I determined in experiment[2–4].

To study the formation of a critical crystal nucleus, we used a biased Monte Carlo method[7,8]. This scheme allows us to compute the equilibrium probability $P(n)$ for the formation of a crystalline cluster of size n. The (Gibbs) free energy of a cluster of size n is given by:

$$G(n) = \text{const.} - \ln[P(n)] \qquad (6)$$

We computed the nucleation barrier as a function of the cluster size n for hard-sphere fluids that were compressed above the coexistence pressure $P_{coex} = 11.67$ (ref. 9). Simulations were performed at reduced pressures $P = 15$, 16 and 17, corresponding to volume fractions of the liquid $\phi_{liq} = 0.5207$, 0.5277 and 0.5343. These state points correspond to the lower range of supersaturations where hard-sphere nucleation has been studied experimentally[2–4]. The reason for selecting this density regime is that at higher supersaturations, many crystal nuclei form simultaneously.

Figure 1 shows the computed excess Gibbs free energy associated with the formation of a cluster of size n in a supercooled liquid. The top of the barrier determines ΔG_{crit} and the critical nucleus size. Comparing our results for ΔG_{crit} with the best experimental estimates, we find that the latter are three times too low[3,4]. One possible source of discrepancy could be that we simulated monodisperse suspensions, whereas the experimental systems have a size polydispersity of approximately 5%. We therefore repeated the simulations for a system with 5% polydispersity. However, we found that the only effect of polydispersity is to shift the coexistence curve. To within the numerical error in ΔG_{crit} ($\pm 1 k_BT$), the monodisperse and polydisperse suspensions have the same nucleation

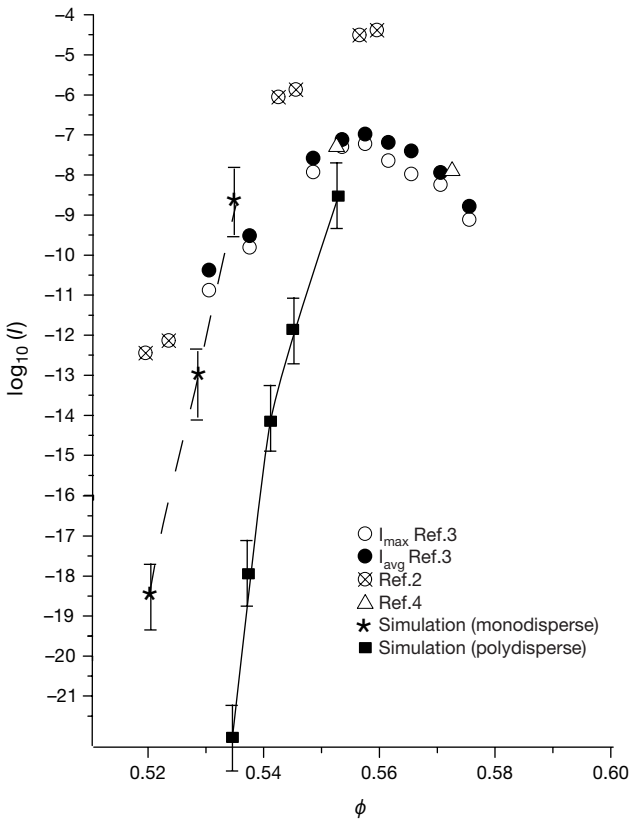

Figure 2 Reduced nucleation rates I as a function of the volume fraction of the metastable liquid. The simulation data for monodisperse colloids are indicated by asterisks—the drawn curve joining the simulation points is meant as a guide to the eye. We also show the experimental results of ref. 2 (crossed circles), ref. 3 (open and filled circles) and ref. 4 (triangles). We also performed simulations on model systems that have the same polydispersity (5%) as the experimental systems. These simulation results are denoted by filled squares. The discrepancy between the latter simulations and experiment is unexpected and significant. Several factors could complicate the comparison with the available experiments: first, the experiments yield a 'time-averaged' nucleation rate that may differ from the steady-state rate that we compute. Secondly, it is conceivable that the experimental systems contain some pre-critical nuclei.

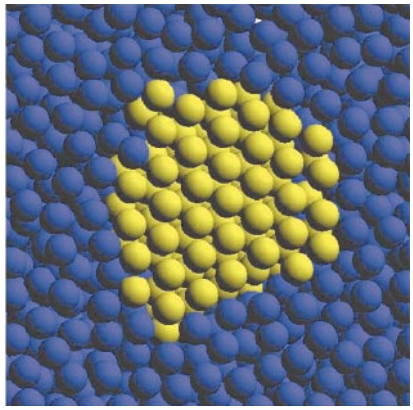

Figure 3 Snapshot of a cross-section of a critical nucleus of a hard-sphere crystal at a liquid volume fraction $\phi = 0.5207$. The figure shows a three-layer-thick slice through the centre of the crystallite. Solid-like particles are shown in yellow, and liquid-like particles in blue. The layers shown in the figure are close-packed hexagonal crystal planes. The stacking shown in this figure happens to be f.c.c.-like (that is, ABC stacking): however, analysis of many such snapshots showed that f.c.c. and h.c.p. stackings were equally likely.

barrier at the same supersaturation (that is, at the same value of $\Delta\mu$). We also compared the computed nucleation barriers with the predictions based on CNT. The dependence of ρ_S and $\Delta\mu$ on P can be accurately computed using the phenomenological equations of state for the solid and fluid phase of hard spheres[10]. For γ we take a recent numerical estimate[11]. The resulting CNT predictions for ΔG_{crit} are 30–50% too low. These deviations are not small. For instance, for a barrier height of $40k_BT$, an error of 30% in ΔG_{crit} implies an error of the order of 10^5 in $\exp(-\Delta G_{crit}/k_BT)$ and the experimental estimate of $\exp(-\Delta G_{crit}/k_BT)$ is in error by a factor of the order of 10^{11}. Although the computed barrier heights are not predicted correctly by CNT, we can still fit our data to the functional form given by CNT (equation (2)). Using $n = 4\pi\rho_S R^3/3$, we can express equation (2) in terms of the cluster size n. The only adjustable parameter in our fit of the simulation data is the effective interfacial free-energy density γ_{eff}. Figure 1 shows that CNT reproduces the functional form of the nucleation barrier, except for very small clusters. The fit yielded the following values: $\gamma_{eff}(P = 15) = 0.699$, $\gamma_{eff}(P = 16) = 0.738$ and $\gamma_{eff}(P = 17) = 0.748$. Again, we find the same answer for the system with 5% polydispersity: that is, at the same supersaturation we obtain the same values for γ_{eff} of the monodisperse and polydisperse samples. We note that the numerical estimate of γ_{eff} is higher than the value deduced from the analysis of experimental nucleation data: the data analysis of refs 3 and 4 suggests that $\gamma_{eff} = 0.5$. As $\Delta G_{crit} \sim \gamma_{eff}^3$, the experimental estimate of ΔG_{crit} is a factor of three too low. If we assume that γ_{eff} depends linearly on pressure, then our simulation results extrapolate to a value of $\gamma \approx 0.62$ at coexistence—in good agreement with the numerical estimate[11]. However, in the regime where nucleation experiments have been performed, we find much larger values for γ_{eff} (between 0.7 and 0.75). CNT fails because it uses the value of γ at coexistence in equation (3) to predict ΔG_{crit}.

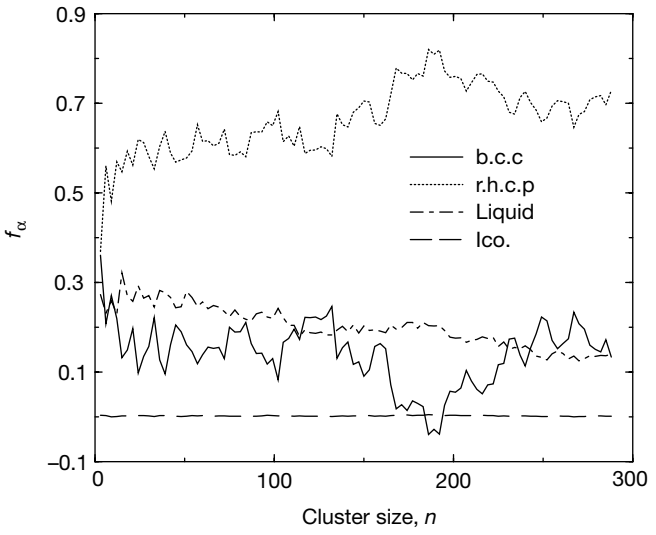

Figure 4 Structure analysis of (pre) critical crystal nuclei. The figure shows the relative weight of the structural signatures for r.h.c.p., b.c.c., icosahedral and liquid-like ordering in hard-sphere crystal nuclei of size n. In order to perform the structural analysis, we first computed the distribution of bond-order parameters for the various pure structures[8]. This is straightforward for liquid structures. In the case of the randomly stacked hexagonal close-packed structure, we determined the signature of a randomly stacked bulk crystal. However, no stable b.c.c. or icosahedral structures exist for monodisperse hard spheres. But we found that we could generate metastable b.c.c. structures for slightly (3%) polydisperse hard-sphere crystals. We computed the b.c.c. signature for this structure. In the case of the icosahedral structure, we computed the relevant bond-order parameter distributions for a particle that was constrained to be in an artificially stabilized icosahedral environment of the correct density. The figure shows that b.c.c. and icosahedral structures play no role in the nucleation process. Small clusters are fairly disordered and have an appreciable liquidlike signature. The figure also shows that the r.h.c.p. signature is dominant for all cluster sizes. However, small crystallites tend to be fairly disordered. In those structures, the b.c.c. and liquid-like signatures become noticeable.

Our simulations allow us to give what we believe to be the first parameter-free estimate of the crystal nucleation rate. To this end, we need to compute the reduced kinetic prefactor κ. It has the following form: $\kappa = Z\rho f_{n_c}/D_0$, where Z is the Zeldovitch factor[1], ρ is the number density of the supersaturated liquid, and f_{n_c} is the addition rate of particles to the critical nucleus. The Zeldovitch factor $Z = [|\Delta G''(n_{crit})|/(2\pi k_BT)]^{1/2}$, where $\Delta G''(n)$ is the second derivative of $\Delta G(n)$, can be obtained directly from the simulation results. We have computed f_{n_c}/D_0 using kinetic Monte Carlo simulations of the hard-sphere suspension[12]. In such simulations, the effect of hydrodynamic interactions between colloids is ignored. However, in line with ref. 13, we correct for this effect by multiplying our Monte Carlo results for f_{n_c} by a factor $\alpha(\phi) \equiv D^s(\phi)/D_0$, where $D^s(\phi)$ is the short-time self-diffusion coefficient at volume fraction ϕ. Several, rather similar, functional forms for $\alpha(\phi)$ have been proposed in the literature. Here we use the phenomenological expression $\alpha(\phi) = (1 - \phi/0.64)^{1.17}$ (ref. 6). When applying the same approach to the computation of the long-time self-diffusion constant, we reproduce the experimental data in the same density range (see ref. 4) to within the statistical error. We estimate that the error in $\ln\kappa$ is ± 1, that is, about the same as the error in $\Delta G_{crit}/k_BT$.

Figure 2 shows our numerical estimate for the reduced nucleation rate I. We have computed I both for a monodisperse suspension and for a suspension with 5% polydispersity. The latter results can be compared directly with the experimental studies of steady-state nucleation[2–4]. As can be seen in Fig. 2, the simulated and experimental curves almost intersect, but for most densities we observe discrepancies of many orders of magnitude. Such discrepancies are both real and a cause for concern, as we estimate that our computed nucleation rates are accurate to within one order of magnitude. We therefore argue that the problem must be with the interpretation of the experiments, and hope that future 'real-space' experiments will provide an explanation for the discrepancy in the computed nucleation rates and barrier heights.

The simulations allow us to address a question that cannot, at present, be answered experimentally: what is the structure of the critical nucleus? Figure 3 shows an example of a snapshot of a critical nucleus observed in our simulations. CNT makes the assumption that the (pre) critical nuclei are effectively spherical, and have the same structure as the stable bulk phase that is nucleating. However, Ostwald[14] pointed out in 1897 that the phase that nucleates need not be the one that is thermodynamically stable. In recent years, several attempts have been made to provide a microscopic explanation for Ostwald's observation[15–17]. Alexander and McTague[15] have argued, on the basis of Landau theory, that in the early stages of crystal nucleation a body-centred cubic (b.c.c.) crystallite should form that would subsequently transform into the stable crystal phase. Indeed, simulations of pre-critical nuclei in a Lennard–Jones ('argon') liquid are found to have b.c.c. structure, rather than the stable face-centred cubic (f.c.c.)—but this f.c.c. phase is only slightly more stable than the hexagonal close packed (h.c.p.) phase[18]. In fact, the f.c.c.–h.c.p. free-energy difference is so small that small hard-sphere crystals will always contain an equilibrium concentration of stacking faults[5,19–21]. It would clearly be interesting to know by what route hard-sphere crystals nucleate: does the small size lift the effective degeneracy between f.c.c. and h.c.p. structures to the extent that one of these dominates, or do hard-sphere crystal nuclei obey the predictions of the Alexander-McTague theory and exhibit a b.c.c. or possibly even icosahedral structure?

To answer this question we analysed the structure of the crystalline nucleus. The stable structure of a bulk hard-sphere solid is f.c.c.[18]. But as the free energy of stacking faults is small[20,21], small crystallites are expected to exhibit random stacking of f.c.c. and

h.c.p. domains. Indeed, direct inspection of the crystal nuclei generated in our simulations show that the critical nucleus is randomly stacked. The next question to ask is if there is any evidence for b.c.c. or icosahedral ordering. To this end, we used the analysis technique of ten Wolde *et al.*[8]. This approach allows us to analyse any cluster structure as a mixture of simple reference structures. We assume that pre-critical nuclei need not have the random-hexagonal close-packed (r.h.c.p.) structure. Rather, we allow for the possibility that the nuclei exhibit a signature characteristic of b.c.c., icosahedral or even liquid-like ordering. Every structure is characterized by a set of numbers $\{f_{bcc}, f_{rhcp}, f_{icos}, f_{liq}\}$, where the value of f_α denotes the relative importance of structure α in the cluster. In Fig. 4 we show the results for f_{bcc}, f_{rhcp}, f_{icos} and f_{liq} as a function of the size of the largest cluster in the system at $P = 15$. The results for $P = 16$ and 17 are qualitatively similar. The figure shows that icosahedral ordering is not observed for any nucleus size. Small clusters still have some b.c.c. or liquid-like signature. But in all cases the r.h.c.p. signature is dominant. The same conclusion holds for the weakly polydisperse crystals that we studied. This observation shows that the simplest of all crystals does not confirm the theoretical prediction that b.c.c. (or icosahedral) (pre)nuclei should be favoured in the crystallization of simple liquids[15–17]. Our finding is also unexpected in the light of the finding that pre-critical Lennard–Jones nuclei have a b.c.c. structure[8]. As the structure of simple liquids is known to be dominated by the short-ranged repulsive forces, we expected that the structure of the pre-critical nucleus in hard-sphere fluids would be b.c.c., as in the Lennard–Jones case.

Random hexagonal close packing (r.h.c.p. stacking) in freshly nucleated colloidal hard-sphere crystals has been observed in several experiments[5,19]. It is usually assumed that the origin of the r.h.c.p. stacking is purely kinetic. Although this may be correct for larger crystals, the present simulation indicates that, in the early stages of nucleation, the r.h.c.p. structure is simply more stable than f.c.c. This phenomenon can be interpreted as a manifestation of Ostwald's 'step rule'[14]. The hard-sphere fluid nucleates into the metastable r.h.c.p. structure. Only later does this metastable structure transform into the stable f.c.c. structure[20,21]. □

Received 21 July; accepted 29 November 2000.

1. Kelton, K. F. *Solid State Physics* Vol. 45, 75–90 (Academic, New York, 1991).
2. Schätzel, K. & Ackerson, B. J. Density fluctuations during crystallization of colloids. *Phys. Rev. E* **48,** 3766–3777 (1993).
3. Harland, J. L. & Van Megen, W. Crystallization kinetics of suspensions of hard colloidal spheres. *Phys. Rev. E* **55,** 3054–3067 (1997).
4. Cheng, Z. *Colloidal Hard Sphere Crystallization and Glass Transition.* Thesis, Princeton Univ. (1998).
5. Zhu, J. *et al.* Crystallization of hard-sphere colloids under microgravity. *Nature* **387,** 883–885 (1997).
6. Van Duijneveldt, J. S. & Lekkerkerker, H. N. W. in *Science and Technology of Crystal Growth* (eds van der Eerden, J. P. & Bruinsma, O. S. L.) 279–290 (Kluwer Academic, Dordrecht, 1995).
7. Van Duijneveldt, J. S. & Frenkel, D. Computer simulation study of free energy barriers in crystal nucleation. *J. Chem. Phys.* **96,** 4655–4668 (1992).
8. Ten Wolde, P. R., Ruiz-Montero, M. J. & Frenkel, D. Numerical evidence for b.c.c. or ordering at the surface of a critical f.c.c. nucleus. *Phys. Rev. Lett.* **75,** 2714–2717 (1995).
9. Hoover, W. G. & Ree, F. H. Melting transition and communal entropy for hard spheres. *J. Chem. Phys.* **49,** 3609–3617 (1968).
10. Hall, K. R. Another hard-sphere equation of state. *J. Chem. Phys.* **57,** 2252–2254 (1970).
11. Davidchack, R. L. & Laird, B. B. Direct calculation of the hard-sphere crystal/melt interfacial free energy. *Phys. Rev. Lett.* **85,** 4751–4754 (2000).
12. Hinsen, K. & Cichocki, B. Dynamic computer simulation of concentrated hard-sphere suspensions. *Physica A* **166,** 473–491 (1990).
13. Medina-Noyola, M. Long-time self-diffusion in concentrated colloidal dispersions. *Phys. Rev. Lett.* **60,** 2705–2708 (1988).
14. Ostwald, W. Studien über die Bildung und Umwandlung fester Körper. *Z. Phys. Chem.* **22,** 289–330 (1897).
15. Alexander, S. & McTague, J. P. Should all crystals be BCC? *Phys. Rev. Lett.* **41,** 702–705 (1978).
16. Klein, W. & Leyvraz, F. Crystalline nucleation in deeply quenched liquids. *Phys. Rev. Lett.* **57,** 2845–2848 (1986).
17. Groh, B. & Mulder, B. M. Why all crystals need not be b.c.c.: symmetry breaking at the liquid–solid transition revisited. *Phys. Rev. E* **59,** 5613–5620 (1999).
18. Bolhuis, P. G., Frenkel, D., Mau, S. C. & Huse, D. A. Entropy difference between the face-centred cubic and hexagonal close-packed crystal structures. *Nature* **388,** 235–237 (1997).
19. Pusey, P. N. *et al.* Structure of crystals of hard colloidal spheres. *Phys. Rev. Lett.* **63,** 2753–2756 (1989).
20. Pronk, S. & Frenkel, D. Can stacking faults in hard-sphere crystals anneal out spontaneously? *J. Chem. Phys.* **110,** 4589–4592 (1999).
21. Mau, S. C. & Huse, D. A. Stacking entropy of hard-sphere crystals. *Phys. Rev. E* **59,** 4396–4401 (1999).
22. Torrie, G. M. & Valleau, J. P. Monte-Carlo free energy estimates using non-Boltzmann sampling: application to the subcritical Lennard-Jones fluid. *Chem. Phys. Lett.* **28,** 578–581 (1974).
23. Geyer, C. J. & Thompson, E. A. Annealing Markov-chain Monte Carlo with applications to ancestral inference. *J. Am. Stat. Assoc.* **90,** 909–920 (1995).

Acknowledgements

We thank H. Lekkerkerker, W. van Megen, W. Kegel, A. van Blaaderen, J. Horbach and B. Smit for a critical reading of the manuscript. This work was supported by the Division of Chemical Sciences (CW) of the Netherlands organization for Scientific Research (NWO). The work of the FOM Institute is part of the research programme of FOM, and is made possible by financial support from the NWO.

Correspondence and requests for materials should be addressed to D.F. (e-mail: frenkel@amolf.nl).

Formation of thermally stable alkylidene layers on a catalytically active surface

El Mamoune Zahidi, Hicham Oudghiri-Hassani & Peter H. McBreen

Départment de Chimie et CERPIC, Université Laval, Québec (PQ), G1K 7P4, Canada

Materials containing organic–inorganic interfaces usually display a combination of molecular and solid-state properties, which are of interest for applications ranging from chemical sensing[1] to microelectronics[2] and catalysis[3]. Thiols—organic compounds carrying a SH group—are widely used to anchor organic layers to gold surfaces[6], because gold is catalytically sufficiently active to replace relatively weak S–H bonds with Au–S bonds, yet too inert to attack C–C and C–H bonds in the organic layer. But although several methods[4–6] of functionalizing the surfaces of semiconductors, oxides and metals are known, it remains difficult to attach a wide range of more complex organic species. Organic layers could, in principle, be formed on the surfaces of metals that are capable of inserting into strong bonds, but such surfaces catalyse the decomposition of organic layers at temperatures above 400 to 600 K, through progressive C–H and C–C bond breaking[7]. Here we report that cycloketones adsorbed on molybdenum carbide, a material known to catalyse a variety of hydrocarbon conversion reactions[8–11], transform into surface-bound alkylidenes stable to above 900 K. We expect that this chemistry can be used to create a wide range of exceptionally stable organic layers on molybdenum carbide.

The experiments were performed by exposing clean molybdenum carbide, in the form of β-Mo_2C, to cycloketones and then probing the surface using infrared reflectance, mass spectrometric thermal desorption, X-ray photoemission (XPS) and chemical reactivity methods. We observed two intense desorption peaks appearing between 900 and 1,200 K, shown in Fig. 1. This feature is common to the data for C_4–C_6 cycloketones, and mass spectrometric calibration data (see Supplementary Information) identify the desorbing species, in each case, as the parent cycloketone molecule. These high-temperature peaks must then arise from ketone-formation reactions, because intact small molecules typically desorb below 400 K. Furthermore, the intermediates for ketone formation must be stable to above 900 K, in contrast to previous observations[7] of the stability of complex organic species on materials as catalytically active[8–11] as β-Mo_2C. Infrared reflectance spectra (Fig. 2a) of a cyclobutanone monolayer adsorbed on β-Mo_2C at 105 K display a carbonyl stretching vibration band at 1,730 cm^{-1} characteristic of a chemisorption bond between the carbonyl oxygen and the surface.